DOI: 10.15849/IJASCA.250330.01

Int. J. Advance Soft Compu. Appl, Vol. 17, No. 1, March 2025
Print ISSN: 2710-1274, Online ISSN: 2074-8523

Rate of Occurrence Estimation in Geometric Processes with Maxwell Distribution: A Comparative Study between Artificial Intelligence and Classical Methods

Adel S. Hussain[1], Kafi D. Pati[2], Ali K. Atiyah[3], and Mohammad A. Tashtoush[4,5*]

[1]IT Department, Amedi Technical Institutes, University of Duhok Polytechnic, Duhok, Iraq.
e-mail: adel.sufyan@dpu.edu.krd
[2]Department of Computer Science, College of Science, University of Duhok, Duhok, Iraq.
e-mail: Kafi.pati@uod.ac.krd
[3]Electronic Computer Centre Department, Al-Iraqi University, Baghdad, Iraq.
e-mail: ali.khalid@aliraqia.edu.iq
[4]Depatrment of Basic Sciences, AL-Huson University College, AL-Balqa Applied University, Salt, Jordan.
[5]Faculty of Education and Arts, Sohar University, Sohar, Oman
e-mail: tashtoushzz@su.edu.om

Abstract

The Geometric Process is a powerful alternative to the Non-Homogeneous Poisson Process for modeling event occurrences across various domains, including engineering, finance, and epidemiology. This study focuses on enhancing parameter estimation for the GP when the time distribution of the first event follows a Maxwell distribution. To achieve this, we applied and compared three estimation techniques: parametric Maximum Likelihood Estimation, non-parametric Modified Moments, and the Firefly Optimization Algorithm. Simulated data from a gas power plant in Mosul was used to assess the performance of these methods. Results demonstrated that all three methods yielded accurate estimates, with FFA outperforming the others in terms of Mean Squared Error. Additionally, the Kolmogorov-Smirnov test validated the data's adherence to the Maxwell distribution, confirming the model's suitability. This study highlights the GP's applicability in real-world scenarios, particularly in reliability engineering and event modeling. However, reliance on simulated data limits the findings, as it may not fully reflect real operational complexities. Future work should extend these methods to diverse datasets and explore different distributional assumptions. The practical implications are significant, as precise parameter estimation can enhance decision-making in engineering processes and resource management. On a broader level, the findings may influence risk assessment approaches and improve operational efficiency in critical infrastructure systems, contributing to societal gains in service reliability and delivery.

Keywords: *Geometric Process, Maxwell Distribution, Maximum Likelihood, Modified Moment Method, Firefly Optimization Algorithm, Artificial Intelligence.*

1 Introduction

Introduced the Geometric Process (GP) as an elegant and straightforward monotone process, perceiving it as an extension of the Renewal Process (RP), [1-2]. This modeling

Received 11 September 2025; Accepted 7 January 2025

framework serves as a potent approach to capture the sequential time intervals between successive event arrivals in a counting process. Let's consider a counting process denoted as a, and let signify the time interval, we will $\{N(t); t \geq 0\}$ to be counting process, and x_i be the time between the $(i-1)^{th}$ andi^{th}events, where $i = 1,2,\ldots$, then:

$$y_i = a^{(i-1)}x_i \ , \ i = 1,2,\ldots,n \tag{1}$$

In this context, we have a series of Independent Identically Distributed (IID) random variables, where the random process is classified as a GP with a parameter a if there exists a real number, where a is referred to as the ratio parameter of the GP [3]. The monotonous behaviour of the GP relies on the value of the ratio parameter a. When $a > 1$, the GP exhibits a decreasing trend; for $a < 1$, it demonstrates an increasing trend. In the special case where $a = 1$, the GP simplifies into a Random Process (RP) [4].

Given the Geometric Process $\{x_i; i = 1,2,....,n\}$ with a ratio parameter a, we can deduce the following:

$$\left.\begin{aligned} E(X_i) \ \frac{\mu}{a^{(i-1)}} \\ var(X_i) = \frac{\sigma^2}{a^{2(i-1)}} \end{aligned}\right\} \tag{2}$$

where $E(x_1) = \mu$ and $var(x_1) = \sigma^2$. Thus a, μ and σ^2 are very important to completely determine the expectation and variance of GP. it is essential to consider the values of a and λ. Numerous research studies have delved into the properties of GP, with notable contributions from [5-7]. These works have explored fundamental characteristics of GP. Addressing the statistical inference challenge for GP, previous studies have made assumptions regarding the distribution of the first occurrence time. In this particular investigation, we adopt the assumption that the distribution of the first occurrence time in GP follows a Maxwell distribution (MAX) with a parameter θ. In Reliability Engineering, the Geometric Process is used to model the time between failures or events in a system [3-4]. In queuing theory, the Geometric Process can be used to model the arrival of customers at a service point or the time between arrivals [5-6].

GP can be applied to model the spread of infectious diseases or the occurrence of rare events in epidemiological studies. Although, In finance, GP can be applied to model the time between stock price movements, the arrival of trading orders, or the occurrence of financial crises [7-10]. In telecommunications, GP can be used to model the arrival of data packets in a network or the time between dropped calls in a cellular network. Furthermore, in biostatistics, GP can be employed to model the time between medical events, such as patient arrivals at a hospital or the occurrence of adverse reactions to a drug [11-12].

This study's primary goal is to estimate parameters of GP when the first occurrence time follows a Maxwell distribution. Section 2 gives comprehensive details on the Maxwell distribution. In Section 3, We derive MLE and MM and Firefly Optimization FFA estimators for the parameters a and λ. Section 4 presents the results of Monte Carlo simulations aimed at comparing the performance of the estimators discussed in Section 5. In Section 6, Present Criteria. In Section 7, a real data set from the Dam power stations in Mosul is implemented, the survival times of patients with brain cancer until death and the dataset, obtained from a real-time command and control system developed by Bell Laboratories. In Section 8, present Discussion of Implications. Finally, Conclusions.

2 Maxwell Distribution

The Maxwell distribution, also known as the Maxwell-Boltzmann Distribution, is a continuous probability distribution commonly used for modelling data sets in the fields of

physics, chemistry, and related areas. This distribution is characterized by increasing failure rates and is suitable for modelling positively skewed data sets. However, it may not be suitable for modelling lifetime data that have both positively and negatively skewed. The distribution function of the Maxwell random variable was introduced by [6]. Let X is a Maxwell distribution of a random variable will be denoted by the parameter λ, we will be indicated $X{\sim}Max(\lambda)$. Thus, $E(X) = 2\lambda\sqrt{\frac{2}{\pi}}$ and $Var(X) = \lambda^2\frac{(3\pi-8)}{\pi}$, for brevity x has the $p.d.f.$ as follow:

$$f(x,\lambda) = \begin{cases} \frac{4}{\sqrt{\pi}\lambda^3}x^2\mathrm{e}^{-(\frac{x}{\lambda})^2} & ; y > 0 \\ 0 & ;\ \text{Otherwise} \end{cases} \tag{3}$$

3 Firefly Algorithm (FFA)

The Firefly Algorithm was initially proposed [13-15]. This method finds optimal solutions to optimization problems by taking cues from the night-time activity and flashing patterns of fireflies. Utilizing variations in light and gravity to direct fireflies toward the brightest and most alluring spots, the goal function is a key component of FFA. To understand FFA better, consider the following principles:

- Light Intensity and Objective Function: The light intensity of a firefly at a given position x in optimization problems is stated by $I(x)$, is directly proportional to the value of the fitness function: $I(x) \propto f(x)$. Essentially, the brightness of a firefly corresponds to the quality of the solution it represents.
- Attractiveness: The intensity of a firefly's gravity, symbolized by β, is proportional to the intensity $I(r)$, of its light intensity. Which, in turn, varies with the distance r_{ij} between firefly i and firefly j. As firefly light intensity decreases with distance due to the absorption of light in the medium.
- Distance and Attractiveness: In the simplest scenario, light intensity $I(r)$ diminishes monotonically and exponentially with distance r. This means that fireflies are more attracted to others that are closer and brighter, as the light intensity diminishes as they move further away.

In summary, the Firefly Algorithm employs the concept of mimicking firefly behavior, where fireflies are drawn to brighter and more attractive locations. In the algorithm, the light intensity of a firefly corresponds to the fitness or quality of a solution, and their attractiveness is influenced by both their own brightness and the distance to other fireflies. This elegant approach has proven to be effective for solving optimization problems and finding optimal solutions.

$$I(r) = I_0 e^{-\gamma r} \tag{4}$$

Where γ expresses the light absorption coefficient, and I_0 represents the original light intensity. It is understood in elementary physics that the intensity of light is inversely proportional to the square of the distance, represented by r, from the source. Therefore, the variation of gravity β with distance r can be defined by:

$$\beta(r) = \beta_0 e^{-\gamma r^2} \tag{5}$$

This formula describes how the attractiveness of a firefly changes as it moves away from the source, with β decreasing as r increases due to the inverse square relationship between light intensity and distance X_i will be as follows:

$$X_{i+1} = X_i^t + \beta_0 e^{-\gamma r_{ij}^2} \left(X_j^t - X_i^t\right) + \alpha_t \epsilon_i^t \quad (6)$$

4 Estimate Parameters for GP

In this section, we focus on the estimation challenges related to the geometric process (GP) when the initial arrival has a Maxwell distribution.

4.1 Maximum Likelihood Estimation (MLE)

Let $\{x_i; i = 1,2,\dots,n\}$ be a random variable of a GP with respect to the parameter a and $x_1 \sim Max(\lambda)$. By considering equation (1), the following likelihood function can be easily written:

$$L(x,\lambda) = \left(\frac{4}{\sqrt{\pi}\lambda^3}\right)^n a^{3\sum_{i=1}^{n}(i-1)} \sum_{i=1}^{n} X_i^2 \, e^{-\frac{1}{\lambda^2}\sum_{i=1}^{n}(a^{i-1}X_i)^2} \quad (7)$$

An alternate expression for the logarithm of the likelihood function in equation (7) is as follows:

$$ln\, L(x,\lambda) = nln\left(\frac{4}{\sqrt{\pi}\lambda^3}\right) + 3\left(\frac{n(n-1)}{2}\right) ln(a) + 2\sum_{i=1}^{n} ln(X_i) - \frac{1}{\lambda^2}\sum_{i=1}^{n}\left(a^{i-1}X_i\right)^2 \quad (8)$$

By taking the derivatives equation (8) with respect to λ and a and setting them to be equal to zero, the probability equations are obtained as follows:

$$\frac{\partial ln\left(L(a,\lambda)\right)}{\partial a} = 0 \;;\; \frac{\partial ln\left(L(a,\lambda)\right)}{\partial \lambda} = 0 \quad (9)$$

So, we get:

$$\frac{\partial \ln L(a,\lambda)}{\partial a} = 3\left(\frac{n(n-1)}{2a}\right) - \frac{2}{\lambda^2}\sum_{i=1}^{n}\left(a^{i-1}X_i\right)(i-1)a^{i-2}X_i \quad (10)$$

$$\frac{\partial \ln L(a,\lambda)}{\partial \lambda} = \frac{-3n}{\lambda} + \frac{2}{\lambda^3}\sum_{i=1}^{n}\left(a^{i-1}X_i\right)^2 \quad (11)$$

By solving (10) and (11), λ equal:

$$\lambda = \sqrt{\frac{2}{3n}\sum_{i=1}^{n}(a^{i-1}x_i)^2} \quad (12)$$

Substituting the value of λ into equation (10) yields:

$$3n(n-1) - \frac{4}{\left(\sqrt{\frac{2}{3n}\sum_{i=1}^{n}\left(a^{i-1}x_i\right)^2}\right)^2}\sum_{i=1}^{n}(i-1)\left(a^{i-1}x_i\right)^2 = 0 \quad (13)$$

Due to the power function of parameter a, the MLE for a, indicated as $\hat{a}_{MLE}$,, cannot be determined directly from the solution of equation (13). A numerical solution is used to determine $\hat{a}_{MLE}$, as shown below:

$$a_{n+1} = a_n - \frac{f(a_n)}{f'(a_n)} \quad (14)$$

f is the objective function specified in equation (13), where. The MLE estimator of λ is produced as follows if we replace the numerical solution of $\hat{a}_{MLE}$, into equation (12):

$$\hat{\lambda}_{MLE} = \sqrt{\frac{2}{3n}\sum_{i=1}^{n}\left(\hat{a}_{MLE}{}^{i-1}x_i\right)^2} \quad (15)$$

The MLE estimators' combined distribution is Asymptotically Normal (AN), as shown in [16-17].

$$\begin{pmatrix}\hat{a}_{MLE}\\ \hat{\lambda}_{MLE}\end{pmatrix} \sim AN\left(\begin{pmatrix}\alpha\\ \lambda\end{pmatrix}, FI^{-1}\right) \quad (16)$$

Where FI^{-1} stands for the Fisher information matrix in reverse. According to the Fisher Information Matrix:

$$FI = \begin{pmatrix} -E\left(\frac{\partial^2 ln(L(a,\lambda))}{\partial a^2}\right) & -E\left(\frac{\partial^2 ln(L(a,\lambda))}{\partial a \partial \lambda}\right) \\ -E\left(\frac{\partial^2 ln(L(a,\lambda))}{\partial \lambda\, \partial a}\right) & -E\left(\frac{\partial^2 ln(L(a,\lambda))}{\partial \lambda^2}\right) \end{pmatrix} \quad (17)$$

Inverse Fisher Information Matrix results are as follows:

$$FI^{-1} = \begin{bmatrix} \frac{21}{44}\frac{a^2}{n^3} & -\frac{3\lambda a}{22n^2} \\ -\frac{3\lambda a}{22n^2} & \frac{\lambda^2}{11n} \end{bmatrix} \quad (18)$$

The asymptotic distribution of $\hat{a}_{MLE}$ and $\hat{\lambda}_{MLE}$ results from equation (16):

$$\left.\begin{aligned} \hat{\alpha}_{MLE} \sim AN\left(\alpha, \frac{21}{44}\frac{a^2}{n^3}\right) \\ \hat{\lambda}_{MLE} \sim AN(\lambda, \frac{\lambda^2}{11n}\ ) \end{aligned}\right\} \quad (19)$$

Furthermore, the estimators $\hat{a}_{MLE}$ and $\hat{\lambda}_{MLE}$ are impartial, consistent, and asymptotically based on the asymptotic variance of each $\hat{a}_{MLE}$ and $\hat{\lambda}_{MLE}$ converges to zero as $n \to \infty$. To determine the fit of GP to the given data, we perform hypothesis testing considering equation (19). $H_0 : a = 1 vs.\ \ H_1 : a \neq 1$, Using the following statistical analysis:

$$U = \frac{n^{\frac{3}{2}}(a_{MLE}-1)}{\sqrt{\frac{21}{44}}\ a_{MLE}}\ , where\ U \sim AN(0,1) \quad (20)$$

4.2 Modified Moment Estimation (MME)

Let $\hat{\lambda}_{MM}$ Lam [18] provided a nonparametric estimator for the parameter λ, to be adjusted moment estimation $\{ y_i; i = 1,2, \dots, n\}$ as:

$$\hat{y}_i = (\hat{a}_{NP})^{i-1} x_i \quad ; i = 1,2, \dots, n \quad (21)$$

Where $\hat{a}_{NP}$ is a nonparametric least squares estimator for GP that estimates the ratio parameter a. This estimator was utilized in [18-19] and was consistent, unbiased, and had a ratio $\hat{a}_{NP}$ distribution that was asymptotically normal so that:

$$\hat{a}_{NP} = exp\left(\frac{6\sum_{i=1}^{n}(n-2i+1)\ ln(x_i)}{n(n-1)(n+1)}\right) \quad (22)$$

Using the sample $\{ x_i;\ i = 1,2, \dots, n\}$ from GP with ratio a, and the Maxwell distribution as a guide:

$$m_i = \frac{1}{n}\sum_{i=1}^{n} \hat{y}_i \quad (23)$$

The initial sample represents a moment and is characterized by the following values:

$$m_i = \frac{1}{n}\sum_{i=1}^{n} (\hat{a}_{NP})^{i-1} x_i \quad (24)$$

Additionally, it shows that the anticipated of the initial population moment of the Maxwell distribution x_i as:

$$\mu = 2\lambda\sqrt{\frac{2}{\pi}} \quad (25)$$

We will obtain the following result by equating the expectation x_i with the sample value of the first moment represented by x_i in equation (22):

$$\hat{\lambda}_{MM} = \frac{\sqrt{\frac{\pi}{2}}}{2n} \sum_{i=1}^{n} (\hat{a}_{NP}{}^{i-1} X_i) \quad (26)$$

4.3 Firefly Algorithm (FFA)

We will estimate the GP by FFA parameters in this part. The essential stages for this approach are shown in the following algorithm:

Step1: Initialization randomly {setting n out of a number n Fireflies, as well as the greatest degree of attraction value β_0, as well as the degree of light intensity (absorption) γ, as well as the phase factor α, and finally the maximum number of repetitions g_{max}.

Step2: Evaluation and computation of the goal function of the greatest brightness I_0 of fireflies using equation (3).

Step3: Once you have identified the optimal firefly, use equations (5) and (6) to progressively determine the relative brightness I and attraction degree β. Next, search for the firefly in the community that has the brightest light, indicating that it is the most ideal firefly.

Step4: Position updating, which is an update of the fireflies' location, is done according to formula (6).

Step5: The algorithm comes to an end at the cycle termination criterion if the termination condition is satisfied; if not, it goes back to step (3). The Firefly optimization algorithm's flowchart looks like this.

5 Simulation

The performance of the FFA, MM, and MLE for parameter a and λ is compared through extensive simulations with 1000 iterations. Subsequently, the simulation study investigated other alternative situations with varying sample sizes ($n = 25, 50$ and 100). The Maxwell parameter was adjusted to 0.5, 1.5, and 2, while the ratio parameter of the engineering process GP was modified to be 0.9, 0.95, 1, 1.05, and 1.10. The MLE, MM, and FFA estimators' performance was assessed using mean square error, or MSE. The findings displayed in table 1 demonstrate that the MSE values of the a estimators drop with increasing sample size. Furthermore, the FFA estimator for a consistently demonstrates superiority over the MM and MLE estimators based on MSE values in all cases presented in Table 1.

Table 1: The simulated RMSE of estimator a and λ, when λ=2, 1.5 and 0.5

		$\lambda = 2$					$\lambda = 1.5$				$\lambda = 0.5$			
a	n		$\hat{a}$		$\hat{\lambda}$		$\hat{a}$		$\hat{\lambda}$		$\hat{a}$		$\hat{\lambda}$	
		Method	Mean	RMSE	Mean	RMSE	Mean	RMSE	Mean	RMSE	Mean	RMSE	Mean	RMSE
0.9	25	MLE	0.8638	0.0011	0.2820	0.0543	0.8725	0.0161	0.2377	0.0399	0.8210	0.0025	0.1194	0.0120
		MM	0.8996	0.0152	9.3220	3.5011	0.9004	0.0009	52.4376	27.4076	0.9005	0.0161	51.4218	15.8405
		FFA	0.4623	0.0138	0.0000	0.0285*	0.9092	0.0003*	2.1543	0.0207*	0.8241	0.0024*	0.0164	0.0153*
	50	MLE	0.0009	0.0004	0.0001	0.0585	0.0009	0.0004	0.0001	0.0241	0.0009	0.0007	0.0002	0.0186
		MM	0.0009	0.0058	3.9514	62.8443	0.0009	0.0057	2.9518	4.3167	0.0009	0.0057	1.0023	31.6517
		FFA	0.0009	0.0012	0.0004	0.0147*	0.0102	0.0003*	0.0102	0.0231*	0.0006	0.0081	0.0000	0.0158*
	100	MLE	0.0001	0.0002	0.0000	0.0607	0.0001	0.0001	0.0000	0.0259	0.0009	0.0005	0.0003	0.0075
		MM	0.0001	0.0021	1.5720	5.3725	0.0001	0.0020	1.1925	9.1936	0.0009	0.0020	3.9306	62.6904
		FFA	0.0001	0.0012	0.0000	0.0281*	0.0000	0.0070	0.0000	0.0258*	0.0009	0.0004*	0.0003	0.0067*
0.8	25	MLE	0.7642	0.0111	1.0984	0.0285	0.9895	0.0012	1.1928	0.0097	0.9406	0.0003	0.5959	0.0030
		MM	0.8000	0.0137	3.5514	0.9577	0.9508	0.0330	1.7216	0.4707	0.9508	0.0332	0.5649	0.2547
		FFA	0.0052	0.0110	1.0458	0.0062*	0.9508	0.0330	1.1029	0.0138	0.9508	0.0332	1.0625	0.0296
	50	MLE	0.9451	0.0002	2.1685	0.1053	0.9626	0.0004	1.4162	0.0027	0.9416	0.0003	0.5676	0.0021
		MM	0.9418	0.0082	2.3604	0.6003	0.9504	0.0124	1.5933	0.3055	0.9498	0.0118	0.5386	0.1965

	FFA	0.9418	0.0082	1.3378	0.0501 *	0.9504	0.0124	1.2442	0.0183	0.9498	0.0118	1.0745	0.0293
100	MLE	0.9505	0.0000	1.8569	0.1045	0.9552	0.0002	1.1692	0.0105	0.9521	0.0001	0.5143	0.0005
	MM	0.9461	0.0039	2.3108	0.5575	0.9502	0.0043	1.5434	0.2084	0.9502	0.0041	0.5133	0.1155
	FFA	0.9641	0.0039	1.3728	0.0442 *	0.9552	0.0043	1.1781	0.0162	0.9502	0.0041	1.0621	0.0297

6 Criteria

Numerous standards have been put out in this study to evaluate how well a model fits the data. Four evaluation criteria are specifically looked at. As shown in the table below:

Table 2: The simulated RMSE of estimator a and λ, when λ=2, 1.5 and 0.5

No.	Criteria	
1	MSE [22]	$\frac{\sum_{i=1}^{n}(X_k-\hat{X}_k)^2}{n}$
2	R-square (R^2) [23]	$1-\frac{\sum_{i=1}^{n}(\hat{X}_k-X_k)^2}{\sum_{i=1}^{n}(X_k-\bar{y}_i)^2}$
3	AIC [24]	$-2\ log\ MLF+2m$
4	MAE [24]	$\frac{\sum_{i=1}^{n}\lvert\hat{X}_k-X_k\rvert}{n-m}$

7 Real data

In this section, three real-world case studies are analyzed to demonstrate the practical applicability and effectiveness of the proposed method.

7.1 Case I (Mosul Gas Power Plant)

The data processing and estimating procedures were demonstrated using a real data set from the Mosul gas power plant, which helped to validate the GP estimators with the Maxwell distribution suggested in this study. This collection consists of 43 data points, identified as U1, that show the intervals between consecutive failures of a gas power plant in Mosul City, Nineveh Governorate, Iraq. The suggested model was then fitted to the observed data $\{x_1, x_2, \dots, x_n\}$ are:

$$\hat{X}_i = \begin{cases} \hat{\mu}_{ML}\ \hat{a}_{ML} & \text{by a GP with ML estimators} \\ \hat{\mu}_{MM}\ \hat{a}_{NP} & \text{by a GP with MM estimators} \\ \hat{\mu}_{MLS}\ \hat{a}_{NP} & \text{by a GP with MLS estimators} \\ \bar{X}_n & \end{cases} \tag{27}$$

where μ represent the estimate of the mean rate of occurrence.
Let $S_k = x_1 + x_2 + \cdots + x_n, k = 1,2, \dots, n,$ then the fitted value of S_k is $\hat{S}_k = \sum_{j=1}^{k} \hat{x}_j$. The plot of may be used to compare the effectiveness of RP, MLE, MM, and FFA estimators for the data set S_k and $\hat{S}_k$ against $k, k = 1,2, \dots, n,$ where:

$$MSE = \frac{1}{n}\sum_{k=1}^{n}\left(X_k - \hat{X}_k\right)^2 \tag{28}$$

To evaluate the data set's underlying distribution $\{x_1, x_2, \dots, x_n\}$, When compatible with a Maxwell distribution, the following linear regression model is taken into account [20-22]:

$$ln\, X_i = \beta - (i-1)\, ln\, a + \varepsilon_i,\ i = 1,2, \dots, n \tag{29}$$

where $\beta = E(ln\, y_i)$, and ε_i refer to the error term, if e^{ε_i} is distributed the Maxwell distribution, the data set $\{x_1, x_2, \dots, x_n\}$ can be modelled using the Maxwell distribution. Then, the ratio parameter a is estimated by equation (20), and ε_i estimated by:

$$\varepsilon_i = ln\, X_i - \beta + (i-1)\, ln\, a \tag{30}$$

Where $\hat{\beta} = \frac{2}{n(n+1)} \sum_{i=1}^{n} (2n - 3i + 2)\, lnx_i$

We use a plot to compare e^{ε_i} our data against the quintiles of the Maxwell distribution in order to determine whether it follows the Maxwell distribution. Take note of how closely the data points resemble a straight line. As a result, we may infer that the 1st, 2nd, and 3rd units of data from the Mosul gas power facility are well described by the Maxwell distribution. Doing a Kolmogorov-Smirnov goodness-of-fit test confirms this finding. (KS = 0.6274 and the related P-Value = 0.2652) on unit data from the Mosul gas power plant, this conclusion is supported.

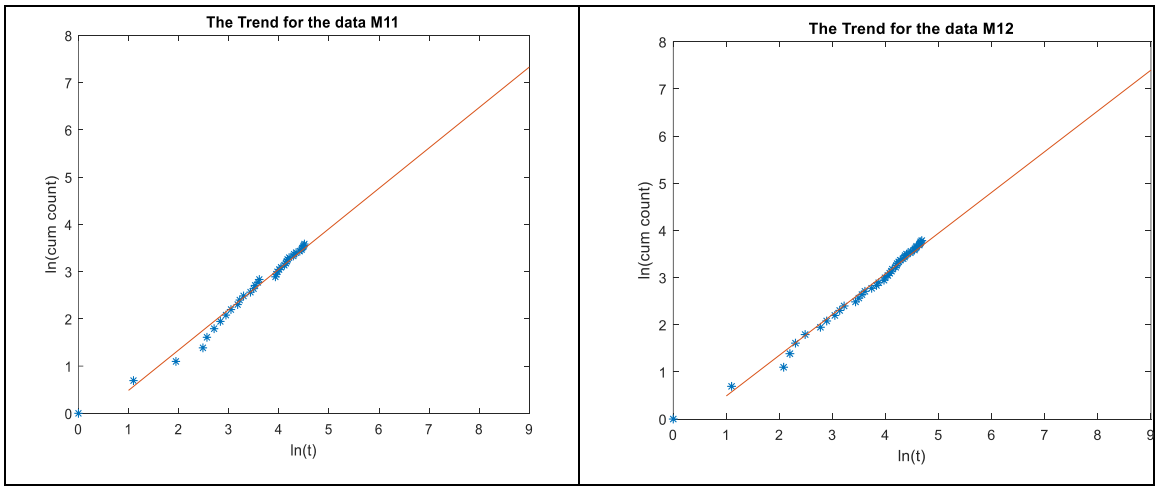

Fig.1. The cumulative data value logarithm is represented by the diffusive form.

The parameters a and λ were estimated using MLE, MM, and FFA estimators, and the MSE, MAE, AIC and R^2 values was calculated for each approach. In addition, the U-test results show that the U_1 data follows the GP distribution when the dataset was modeled using the GP with Maxwell distribution, and these results are presented in Table 3.

Table 3: Parameter, MSE, MAE, AIC, R^2 and U-test estimations.

Unite	n	Method	$\hat{a}$	$\hat{\lambda}$	Criteria				Stat. Test	
					MSE	AIC	MAE	R^2	U	P-value
U1	43	MLE	1.0366	0.9303	0.4609	36.6950	0.1425	0.3650	0.6274	0.2652
		MM	1.0412	0.6580	0.4676	37.7075	0.1450	0.5124		
		RP	1	1.2467	0.4968	39.6252	0.4267	0.4244		
		FFA	0.9973	0.0001	0.2224	26.1866	0.1311	0.3474		

From Fig. 2 can be seen, that the GP with the MLE, MM and FFA estimator more fairly follow real data than the RP.

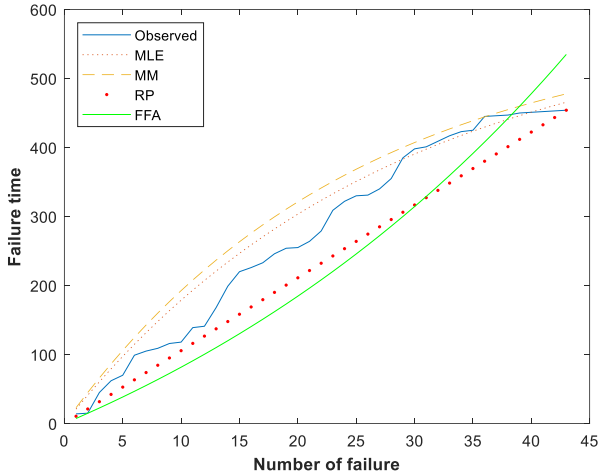

Figure 2. Number of failures plot against S_k and $\hat{S}_k$

7.2 Case II (Survival Times of Patients with Brain Cancer until Death)

The actual data represents the survival times of patients with brain cancer until death, which were obtained from the patient registry at the Imam Hussein (peace be upon him) Centre for the Treatment of Oncology and Blood Diseases in the Holy Governorate of Karbala, if a random sample of 100 patients was taken and their survival period was determined. Until death (in years) [23-25].

The parameters a and λ were estimated using MLE, MM, and FFA estimators, and the MSE, MAE, AIC and R^2 values was calculated for each approach. In addition, the U-test results show that the U_2 data follows the GP distribution when the dataset was modelled using the GP with Maxwell distribution, and these results are presented in Table 4.

Table 4: Parameter, MSE, MAE, AIC, R^2 and U_2-test estimations.

Unite	n	Method	$\hat{a}$	$\hat{\lambda}$	Criteria				Stat. Test	
					MSE	AIC	MAE	R^2	U	P-value
U_2	100	MLE	2.0366	1.9303	1.4609	37.6950	1.1425	1.3650	0.4274	0.1652
		MM	2.0412	1.7580	1.4676	38.7075	1.1450	1.5124		
		RP	1.2	2.2467	1.4968	40.6252	1.4267	1.4244		
		FFA	1.9973	0.0004	1.2224	27.1866	1.1311	1.3474		

Figure 3 demonstrates that the GP model, when combined with the MLE, MM, and FFA estimators, aligns more closely with the real data compared to the RP estimator, highlighting its superior performance in capturing the underlying trends.

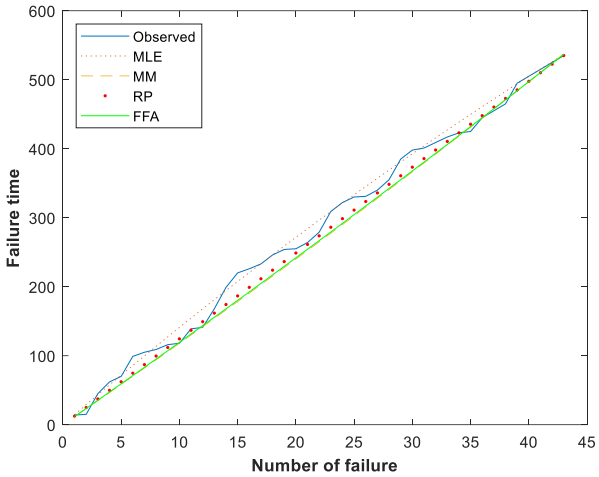

Figure 3. Number of failures plot

7.3 Case III (Real-Time Command and Control System Developed by Bell Laboratories)

In this section, real-world data is utilized to evaluate the performance criteria of the proposed model. The dataset, obtained from a real-time command and control system developed by Bell Laboratories, serves as the basis for comparing the model's goodness of fit. The evaluation results are summarized in the table below.

Table 5: Parameter, MSE, MAE, AIC, R^2 and U_3-test estimations.

Unite	**Size n**	**Method**	$\hat{a}$	$\hat{\lambda}$	Criteria				**Stat. Test**	
					MSE	**AIC**	**MAE**	$\boldsymbol{R^2}$	**U**	**P-value**
U_3	40	**MLE**	2.0363	1.8203	2.4609	36.6950	2.1425	2.3651	0.2274	0.0652
		MM	2.0415	1.6480	2.4676	39.7075	2.1450	2.5125		
		RP	1.5	2.1567	2.4968	35.6252	2.0267	2.4245		
		FFA	1.9965	0.1104	2.2224	25.1866	1.0311	2.3474		

Figure 4 demonstrates that the GP model, when combined with the MLE, MM, and FFA estimators, aligns more closely with the real data compared to the RP estimator, highlighting its superior performance in capturing the underlying trends.

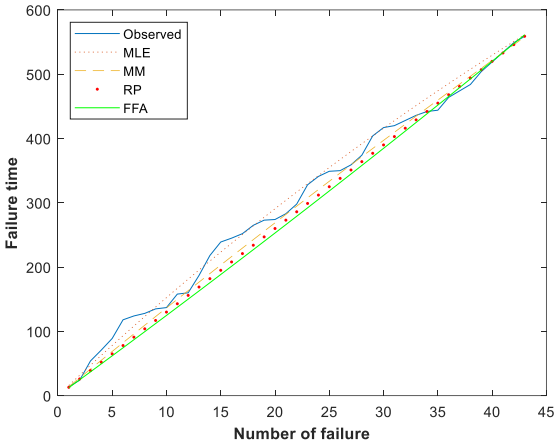

Figure 4. Number of failures plot

This paper compared the results of the GP model employing the Maxwell distribution with actual performance data in three cases. FFA estimator outperformed here with less Mean Squared Error (MSE) and more R-squared values as compared to MLE and MM in Case I (failure data). The GP model considered was found to perform better than the inhomogeneous Poisson process in Case II (survival times of brain cancer patients) and FFA estimator provide the best fit with the help of MSE and AIC. Also, in Case III having command and control system data the FFA estimator provided best performance measure of MSE and MAE. The findings presented in Tables 3, 4, and 5 provide substantial evidence for validity of the proposed FFA estimator in the parameter estimation of GP models improving its solutions adoption in various fields.

8 Discussion of Implications

In this section, we provide a comprehensive analysis of the scenarios, which are systematically categorized into three distinct parts to illustrate the broader implications and insights derived from the study.

8.1 Reliability Engineering in Power Plants

Reliability of equipment is critical in a gas power plant in order to support continuous energy production. Using distribution of intervals between failure of critical components such as turbines and generators, Maxwell coupled with GP framework provides a good fit. Using historical data, trends like increased time between failures could be observed and deduced to be as a result of equipment degradation of improved maintenance strategies. By virtue of the GP model, it is possible to predict future failure times to a t, which can be used for the proper scheduling of maintenance intervals. This helps to avoid prolonged machines inactivity, lower costs and increase operational performance. For instance, if the model predicts that failure rate within the next month will be high in particular equipment; maintenance can be scheduled to avoid equipment breakdowns.

8.2 Resource Management in Telecommunications

Based on the characteristics of telecommunications networks, incoming data packets can be modeled by counting processes the analysis of inter-arrival times which is important for achieving network benefits. The use of the GP framework together with Maxwell distribution means that instead of waiting for the packets to arrive at a certain moment and

analyses packet arrival times to look for a bottleneck, network engineers can use the same to discover that a bottleneck exists romance.
By applying the GP framework with the Maxwell distribution, network engineers can identify patterns in packet arrival times and detect potential bottlenecks. For instance, suppose the model shows that packet frequency increases during rush hour; then it might suggest that a new bandwidth or infrastructure is required.
These capabilities resources also allow for an optimal resource planning by being to provide a predictive based future importance. Expected traffic is another consideration that can be handled by allocating additional bandwidth and servers before peak time to avoid added latency and improve user experience at times of increased load.

8.3 Epidemiological Studies

In epidemiological investigations, it is important to establish the time periods between cases of contagious diseases so as to develop good control measures.
Ultimate spacing of incidents including COVID-19 can then be modeled by employing the GP with Maxwell distribution. The method used in this approach enables the determination of patterns of spread of diseases; and evaluating the impact of measures placed to check its spread.
However, a short period between cases may point to a surge of the numbers, and these require immediate reactions like testing, launches of vaccination drives or enhanced measures towards containing the virus. On the other hand, an extension of periods may be explained by effective treatments that enable the gradual easing of restrictions. Such an approach helps make appropriate decisions promptly and in accordance with statistical data to prevent diseases efficiently.
In each of these contexts, there is direct immediate application from the GP with Maxwell distribution and learning these notations yield useful insights that can help enhance reliability, efficiency and responsiveness across various applications and disciplines. In this respect, organizations can use sophisticated modeling approaches to create value, optimize operations, improve utilization of resources and, consequently, improve results in engineering, telecommunications, and public health.

9 Conclusion

This study investigates the estimation of the frequency of occurrence of the GP when the time distribution of the first occurrence follows the Maxwell distribution. Three different methods for estimating the parameters of the GP were proposed and compared, namely the parametric MLE, the non-parametric MM and FFA. The simulation results and the analysis of real data have shown that the FFA estimator outperforms the MM and MLE estimators in terms of accuracy and efficiency. In addition, analysis of a real data set from a gas-fired power plant in Mosul showed that the GP model with the Maxwell distribution provides a better fit to the data than the inhomogeneous Poisson process. We also developed a test statistic to check whether the data fit a GP. Our results suggest that the GP model with the Maxwell distribution is a viable approach for modeling events in different domains.

Based on the future work needed to further the GP with the Maxwell distribution, I suggest using various datasets from real-life application areas such as telecommunications and/or healthcare to increase generalization. A time comparison can reveal temporal trends and analysis with an alternate distribution such as Weibull, Log-Normal, or the use of Hybrid Models may provide a deeper insight of the system under analysis.

Use in machine learning and Bayesian inference would help enhance parameters, results forecasting, and accuracy. Internal and external cross-validation coupled with intense cooperation with practitioners in the respective industries would guarantee the credibility of the findings and their practical relevance, respectively, thereby bringing efficiency to the calculations made in various applications.

ACKNOWLEDGEMENTS

The authors are very grateful to the Al-Iraqi University for providing access which allows for more accurate data collection and improved the quality of this work.

References

[1] W. Hu, P. Westerlund, P. Hilber, C. Chen, and Z. Yang, (2022). "A general model, estimation, and procedure for modeling recurrent failure process of high-voltage circuit breakers considering multivariate impacts," *Reliab. Eng. Syst. Saf.*, vol. 220, p. 108276.

[2] C. Li, (2021). "Sequential Modelling and Inference of High-frequency Limit Order Book with State-space Models and Monte Carlo Algorithms." *University of Cambridge*.

[3] S. Ahamad, (2021). "Some studies on performability analysis of safety critical systems," *Comput. Sci. Rev.*, vol. 39, p. 100319.

[4] V. Chetlapalli, H. Agrawal, K. Iyer, M. Gregory, V. Potdar, and R. Nejabati, (2022). "Performance evaluation of IoT networks: A product density approach," *Comput. Commun.*, vol. 186, pp. 65–79.

[5] Y. Wu, S. Tait, A. Nichols, and J. Raja, (2021). "Simulation of railway drainage asset service condition degradation in the UK using a Markov chain–based approach," *J. Infrastruct. Syst.*, vol. 27, no. 3, p. 4021023.

[6] H. Lee and T. Lee, (2018). "Markov decision process model for patient admission decision at an emergency department under a surge demand," vol. 30, pp. 98–122.

[7] S. Suman, S. Khan, S. Das, and S. Chand, (2016). "Slope stability analysis using artificial intelligence techniques," *Nat. Hazards*, vol. 84, pp. 727–748.

[8] D. Wang et al., (2017). "System impairment compensation in coherent optical communications by using a bio-inspired detector based on artificial neural network and genetic algorithm," *Opt. Commun.*, vol. 399, pp. 1–12.

[9] S. Ali, (2015)."Mixture of the inverse Rayleigh distribution: Properties and estimation in a Bayesian framework," *Appl. Math. Model.*, vol. 39, no. 2, pp. 515–530.

[10] H. Zureigat, M. Tashtoush, A. Jameel, E. Az- Zo'bi, M. Alomare,(2023). "A solution of the complex fuzzy heat equation in terms of complex Dirichlet conditions using a modified Crank-Nicolson method". *Advances in Mathematical Physics*, vol, Article ID 6505227.

[11] Hussain, A. S., Oraibi, Y. A., Sulaiman, M. S., & Abdulghafour, A. S. (2024). Parameters Estimation of a Proposed Non-Homogeneous Poisson Process and Estimation of the Reliability Function Using the Gompertz Process: A Comparative Analysis of Artificially Intelligent and Traditional Methods: nonhomogenous poisson process with intelligent. *Iraqi Journal For Computer Science and Mathematics*, 5(2), 36-47.

[12] N. Shirawia, A., Kherd, S., Bamsaoud, A., Jassar,(2024). "Dejdumrong Collocation Approach and Operational Matrix for a Class of Second-Order Delay IVPs: Error

analysis and Applications". *WSEAS Transactions on Mathematics*, vol. 23, Article ID 49, 467-479.

[13] D. Cox and P. Lewis, (1966). “The statistical analysis of series of events,”

[14] T. Chai and R. Draxler, (2014). “Root mean square error (RMSE) or mean absolute error (MAE),” *Geosci. Model Dev. Discuss.*, vol. 7, no. 1, pp. 1525–1534.

[15] U. Ilhan,(2019). “Statistical inference for geometric process with the inverse Rayleigh distribution,” *Sigma J. Eng. Nat. Sci.*, vol. 37, no. 3, pp. 871–882.

[16] S. Chupradit, et al.(2023). "Modeling and Optimizing the Charge of Electric Vehicles with Genetic Algorithm in the Presence of Renewable Energy Sources". *Journal of Operation and Automation in Power Engineering*, vol. 11, no. 1, pp. 33-38. https://doi.org/10.22098/joape.2023.9970.1707

[17] G. Srinivasa Rao, S. Mbwambo, and A. Pak, (2021). “Estimation of multicomponent stress-strength reliability from exponentiated inverse Rayleigh distribution,” *J. Stat. Manag. Syst.*, vol. 24, no. 3, pp. 499–519.

[18] Hussain, A., Oraibi, Y., Mashikhin, Z., Jameel, A., Tashtoush, M., & Az-Zo’Bi, E. A. (2025). "New Software Reliability Growth Model: Piratical Swarm Optimization-Based Parameter Estimation in Environments with Uncertainty and Dependent Failures". *Statistics, Optimization & Information Computing*, *13*(1), 209-221. https://doi.org/10.19139/soic-2310-5070-2109

[19] R. Ghosh, N. Sinha, S. Biswas, and S. Phadikar, (2019). “A modified grey wolf optimization based feature selection method from EEG for silent speech classification,” *J. Inf. Optim. Sci.*, vol. 40, no. 8, pp. 1639–1652, doi: 10.1080/02522667.2019.1703262

[20] S. Chupradit, et al. (2022). "A Multi-Objective Mathematical Model for the Population-Based Transportation Network Planning. *Industrial Engineering & Management Systems*", vol. 21, no. 2, pp. 322-331. https://doi.org/10.7232/iems.2022.21.2.322

[21] SH, A., Fatah, K. S., & Sulaiman, M. S. (2023). Estimating the Rate of Occurrence of Exponential Process Using Intelligence and Classical Methods with Application. *Palestine Journal of Mathematics*, 12.

[22] M. Stehlík, (2006). “Exact likelihood ratio scale and homogeneity testing of some loss processes,” Stat. Probab. Lett., vol. 76, no. 1, pp. 19–26, 2006

[23] N. Anjum, M., Haque, M. A., & Ahmad, (2013).“Analysis and ranking of software reliability models based on weighted criteria value,” *Int. J. Inf. Technol. Comput. Sci*, vol. 19, no. 6, pp. 1–14.

[24] Az-Zo’bi, E., Rahman, R., Akinyemi, L. Ahmad, H., Tashtoush, M., Mahariq, I. (2024). Novel topological, non-topological, and more solitons of the generalized cubic p-system describing isothermal flux. *Optical and Quantum Electronics*, *56*(1), Article ID 84, 1-16. https://doi.org/10.1007/s11082-023-05642-7

[25] Singh, S. V., Sharma, V. K., & Singh, S. K. (2022). Inferences for two parameter Teissier distribution in case of fuzzy progressively censored data. *Reliability: Theory & Applications*, 17(4), 559-573.

Notes on Contributors

Adel S. Hussain is Assistant Professor at the Department of IT, Amedi Technical Institutes, University of Duhok Polytechnic, Duhok, Iraq. His main teaching and research interests include Artificial Intelligence, Stochastic Process. He has published several research articles in international journals of mathematics.

Kafi D. Pati is Assistant Professor at the Department of Computer Science, College of Science, University of Duhok, Duhok, Iraq. Her main teaching and research interests include Applied Statistics, Computer Science and Fuzzy Logic. He has published several research articles in international journals of mathematics.

Ali K. Atiyah is a Lecture at the Electronic Computer Centre Department, Al-Iraqi University, Baghdad, Iraq. His main teaching and research interests include Numerical Analysis, Fuzzy Logic. He has published several research articles in international journals of mathematics.

Mohammad A. Tashtoush is an Assistant Professor. He received his Ph.D. in Curriculum and Instruction in Mathematics Education, M. Sc. and B. Sc. Degrees in Mathematics. His research interest includes a range of interdisciplinary areas: Applied Mathematics, Mathematical Physics, Statistics, Curriculum and Instruction, ChatGPT, AI, ICT, and IoT in Education, Teaching Methods, TIMSS, PISA and STEM. He has published more than 55 peer-reviewed articles in different journals indexed in international global databases; he is a reviewer for more than 27 indexed journals, member of the editorial board for 3 journals and editor for the International Journal of education and teaching zone.